Shell-model calculations of isovector electromagnetic transitions and Gamow-Teller beta decays in the $N \simeq 28$ region

Atsushi Yokoyama
Laboratory of Physics, School of Medicine, Teikyo University, Hachioji, Tokyo 192, Japan

Hisashi Horie
Laboratory of Physics, Kanto Gakuin University, Yokohama, Kanagawa 236, Japan
(Received 3 February 1988)

Isovector $E2$ and $M1$ transitions from isobaric analog states of the $N=29$ isotones to low-lying states in the $N=28$ isotones are discussed by making use of the shell model. The $f_{7/2}^{n}{}^{-1}j$ and the $f_{7/2}^{n}+f_{7/2}^{n}{}^{-1}j$ configurations are assumed for the $N=29$ and $N=28$ isotones, respectively, where j denotes one of the $p_{3/2}$, $p_{1/2}$, and $f_{5/2}$ orbits. First, the model space is restricted to $j=p_{3/2}$ only, and it is extended to include all the $p_{3/2}$, $p_{1/2}$, and $f_{5/2}$ orbits, in order to study stepwise the role of the various wave function components. For the isovector E2 transitions, it is confirmed that the major components of the wave functions play a decisive role for the allowed transitions in the single-particle shell model and the use of the good isospin wave functions is indispensable for the forbidden ones. For the isovector $M1$ transitions, it is shown that the spin-nonflip $f_{7/2}\rightarrow f_{7/2}$ transition, which is introduced by the neutron-excited components in the wave functions of the $N=28$ isotones, plays a very significant role: It gives rise to the important cancellation which is responsible for the strong suppression of the $M1$ transition strength in comparison with the simple shell-model prediction, and it becomes the leading term in the l- and j-forbidden $M1$ transitions. Similar discussion holds for the Gamow-Teller beta decays between the levels of the $N=28$ and $N=29$ nuclei.

I. INTRODUCTION

Shell-model calculations of the $N \simeq 28$ nuclei have been carried out systematically by assuming one-particle excitations from the $f_{7/2}$ to the upper fp shell.[1,2] In the early stage, only the $p_{3/2}$ orbit was taken into account, i.e., the $f_{7/2}^{n}+f_{7/2}^{n}{}^{-1}p_{3/2}$ configurations,[1] where n is the number of nucleons outside ^{40}Ca, namely $n=A-40$, with A being the mass number of the nuclei. Subsequently, the model space was extended to include all the remaining orbits of the fp shell, i.e., the $f_{7/2}^{n}+f_{7/2}^{n}{}^{-1}(p_{3/2}, p_{1/2}, f_{5/2})^{1}$ configurations.[2] In these calculations, the neutron-excited configurations which were neglected in the previous shell-model calculations[3-5] of the $N=28$ isotones have been investigated by including them explicitly in the model space. In order to minimize ambiguities, the effective interactions relevant to each model space were derived empirically by the least-squares fitting procedure. It has been shown[1,2] that such configurations are indispensable in interpreting various spectroscopic properties of the $N \simeq 28$ isotones, e.g., the high-spin states of the $N=28$ isotones.[1] Since the isovector $M1$ transitions and the Gamow-Teller (GT) beta decays in the $N \simeq 28$ region are expected to be sensitive to the admixture of the neutron-excited components in the shell-model wave functions, the transitions of the isovector type seem to be suitable for investigating the effects of the neutron-excited configurations on the transition matrix elements. The purpose of this paper is to present systematic calculations of the isovector $E2$ and $M1$ transitions and the GT beta decay matrix elements between the levels in the $N=28$ and $N=29$ nuclei, by using the same models we have proposed so far.[1,2]

There have been a number of theoretical works[6-9] on the $M1$ transition strength from the isobaric analog state to the low-lying state which has the largest spectroscopic factor in proton stripping reactions. It is well known that such a low-lying state is no longer the pure antianalog state but contains a considerable amount of the core-polarized state (CPS) generated by recoupling both the isospin and the angular momentum of the core state. It should be mentioned here that the CPS can be obtained from the neutron-excited configuration. The $M1$ matrix elements connecting the analog with these two basis states cancel each other, and therefore the strong suppression of the $M1$ transition strength can be obtained, compared with the prediction assuming the pure analog to antianalog $M1$ transition. Most theoretical discussions, however, were made either for the simplest nucleus like ^{49}Sc or by using an oversimplified shell model. Exceptions might be the calculations by Osnes and Warke[10] for ^{51}V and by Prakash[11] for ^{52}Cr, in which they have examined the role of isospin on the isovector transition matrix elements using the shell-model wave functions with and without correct isospin. The l- and j-forbidden transitions in ^{51}V have also been discussed in Ref. 10, which in general give us a sensitive test for the shell-model wave functions obtained with the extended model spaces. The CPS mentioned before, which plays a crucial role in the $M1$ matrix elements, was not taken into account in their[10,11] calculations, however. It would

be, therefore, interesting to calculate the transition strengths in ^{51}V and ^{52}Cr by using our models in which the neutron-excited configurations are explicitly included and hence the CPS is taken into account. Comparison of the calculations with and without the neutron-excited configurations would provide information on how the CPS works in the isovector transitions in the relatively complicated nuclei. Since it is expected that the spin-flip components such as the $f_{7/2}\rightarrow f_{5/2}$ play an important role in the $M1$ matrix elements, the calculations with our second model of the $f_{7/2}^{n}+f_{7/2}^{n-1}(p_{3/2},p_{1/2},f_{5/2})^{1}$ configurations are carried out.

Isospin structure of the basis functions is first summarized, and the assumptions made for the transition operators and the wave functions are presented in Sec. II. Results of the calculations are given in Sec. III and discussed for an individual nucleus by comparing with the experimental data and partly with the previous calculations. In Sec. IV we summarize the present calculations and give concluding remarks.

II. SHELL MODEL

When both eight neutrons and p protons are filling the $f_{7/2}$ shell outside an inert ^{40}Ca core, the total isospin T and its third component T_z of the low-lying states are defined uniquely by $T=T_z=4-p/2$, and the basis functions for the $N=28$ isotones generated by such configurations are given by

$$|f_{7/2}^{p+8};\alpha TT_zJ\rangle \ . \tag{1}$$

Here, J is the total angular momentum and α represents any additional quantum numbers. If a particle is promoted from the $f_{7/2}$ shell to an upper j shell, then the basis functions with good isospin generated by such configurations can be obtained by coupling the particle to the $f_{7/2}^{p+7}$ core states;

$$|f_{7/2}^{p+7}\alpha_1T_1J_1,j;TT_zJ\rangle \ , \tag{2}$$

where T_1 is the isospin and J_1 is the total angular momentum, both of which are allowed values for the core states. It is obvious due to the triangular condition that two values, $T+\frac{1}{2}$ and $T-\frac{1}{2}$, are generally allowed for T_1. For the $T_1=T+\frac{1}{2}$ state, Eq. (2) consists of two components in the proton-neutron formalism: One involves proton excitation and the other neutron excitation. By using the Clebsch-Gordan (CG) coefficients of isospin, it is given by

$$|f_{7/2}^{p+7}T_1=T+\tfrac{1}{2},j;TT_z=T\rangle=\left[\frac{9-p}{10-p}\right]^{1/2}|[(\pi f_{7/2})^{p-1}(\nu f_{7/2})^{8};T_1=T_{1z}=T+\tfrac{1}{2}],\pi j\rangle$$
$$-\left[\frac{1}{10-p}\right]^{1/2}|[(\pi f_{7/2})^{p}(\nu f_{7/2})^{7};T_1=T+\tfrac{1}{2}T_{1z}=T-\tfrac{1}{2}],\nu j\rangle \ . \tag{3}$$

Here, π and ν stand for the protons and neutrons, respectively, T_{1z} is the third component of T_1, and only the coupling concerning isospin is shown explicitly for the sake of simplicity. In the calculations of Refs. 3 and 4, only the first term of Eq. (3) was taken into account, while the second term of Eq. (3) was considered in Refs. 5 and 10 in order to have the wave functions with correct isospin by using an isospin projection method. For the $T_1=T-\frac{1}{2}$ state, on the other hand, we have only the neutron excitation;

$$|f_{7/2}^{p+7}T_1=T-\tfrac{1}{2},j;TT_z=T\rangle$$
$$=|[(\pi f_{7/2})^{p}(\nu f_{7/2})^{7}T_1=T_{1z}=T-\tfrac{1}{2}],\nu j\rangle \ . \tag{4}$$

It should be noticed that the core states with the same isospin T_1, i.e., the first and second terms of Eq. (3), must have exactly the same J_1 structure, whereas the core states with the different T_1, i.e., the second term of Eqs. (3) and (4), have entirely different J_1 structure. The state with $T_1=T-\frac{1}{2}$ and $J_1^{\pi}=1^{+}$ is often referred to as the core-polarized state. Effects of the neutron-excited states given by Eq. (4) have been investigated in our previous works,[1,2] and study of the effects on the isovector transitions is the main subject for the present calculations.

The basis functions for the $N=29$ isotones are generated by the configurations with the $p-1$ protons and eight neutrons in the $f_{7/2}$ shell and with one neutron in the upper j shell;

$$|f_{7/2}^{p+7}\alpha_1T_1=T+\tfrac{1}{2}J_1,j;T+1T_z=T+1J\rangle \ . \tag{5}$$

By using the isospin lowering operator or the isospin CG coefficients, we can define an isobaric analog state of (5);

$$|f_{7/2}^{p+7}\alpha_1T_1=T+\tfrac{1}{2}J_1,j;T+1T_z=TJ\rangle=\left[\frac{1}{10-p}\right]^{1/2}|[(\pi f_{7/2})^{p-1}(\nu f_{7/2})^{8};T_1=T_{1z}=T+\tfrac{1}{2}],\pi j\rangle$$
$$+\left[\frac{9-p}{10-p}\right]^{1/2}|[(\pi f_{7/2})^{p}(\nu f_{7/2})^{7};T_1=T+\tfrac{1}{2}T_{1z}=T-1/2],\nu j\rangle \ . \tag{6}$$

It is clear that state (3) is orthogonal to state (6), and thus state (3) is usually called an antianalog state.

The one-particle operators for the $E2$ and $M1$ transitions are given by

$$O(E2)^{(2)}_{\mu}=\sum_k e_k r_k^2 Y^{(2)}_{\mu}(\Theta_k) \tag{7}$$

and

$$O(M1)^{(1)}_{\mu}=\left[\frac{3}{4\pi}\right]^{1/2}\sum_k [\tfrac{1}{2}g_s(k)\sigma^{(1)}_{\mu}(k)+g_l(k)l^{(1)}_{\mu}(k)] , \tag{8}$$

respectively. Here, $Y^{(2)}$ is the spherical harmonic of order 2, $\sigma^{(1)}$ is the Pauli spin operator and $l^{(1)}$ is the orbital angular momentum operator, and k runs all over the nucleons. If we introduce the tensor operator $\tau^{(1)}_{\nu}$ for isospin, the one-particle transition operators can be decomposed into isoscalar and isovector components. By using $\tau^{(1)}_0=2t_z$, where t_z is the third component of the isospin operator, the isovector operators for the $E2$ and $M1$ transitions are given by

$$O(E2)^{(\lambda=2,\kappa=1)}_{\mu\ 0}=\tfrac{1}{2}(e_{\nu}-e_{\pi})\sum_k r_k^2 Y^{(2)}_{\mu}(\Theta_k)\tau^{(1)}_0(k) , \tag{9}$$

$$O(M1)^{(\lambda=1,\kappa=1)}_{\mu\ 0}=\frac{1}{2}\left[\frac{3}{4\pi}\right]^{1/2}\sum_k [\tfrac{1}{2}(g_s^{\nu}-g_s^{\pi})\sigma^{(1)}_{\mu}(k)+(g_l^{\nu}-g_l^{\pi})l^{(1)}_{\mu}(k)]\tau^{(1)}_0(k) . \tag{10}$$

The $E2$ matrix element is calculated by using the harmonic oscillator wave functions with the oscillator constant $\nu=m\omega/\hbar=0.96A^{-1/3}$ fm^{-2}, where A is the mass number of a nucleus. Effective charges, $1.5e$ for a proton and $1.0e$ for a neutron, are assumed. For the $M1$ operator, we use the free-nucleon g factors; $g_s=5.5855$ and $g_l=1.0$ for a proton, and $g_s=-3.8263$ and $g_l=0$ for a neutron in unit of μ_N.

The transition operators for the Fermi and Gamow-Teller beta decays are given by

$$O(F)^{(\lambda=0,\kappa=1)}_{\pm 1}=\sum_k t_{\pm}(k)=T_{\pm} \tag{11}$$

and

$$O(\mathrm{GT})^{(\lambda=1,\kappa=1)}_{\mu\ \pm 1}=\sum_k \sigma^{(1)}_{\mu}t_{\pm}(k)=\mp\frac{1}{\sqrt{2}}\sum_k \sigma^{(1)}_{\mu}(k)\tau^{(1)}_{\pm 1}(k) , \tag{12}$$

respectively. Here, we use the relation between the isospin raising (lowering) operator and the isotensor operators;

$$t_{\pm}=t_x\pm it_y=\mp\frac{1}{\sqrt{2}}\tau^{(1)}_{\pm 1} . \tag{13}$$

The ft value is calculated[12] by

$$ft=C/[B(F)+|g_A/g_V|^2B(\mathrm{GT})] , \tag{14}$$

where $B(F)$ and $B(\mathrm{GT})$ are the transition rates for the Fermi and the Gamow-Teller decays, respectively. The $B(k)$ is given by

$$B(k)=|\langle f\|O(k)\|i\rangle|^2/(2J_i+1) , \tag{15}$$

where k denotes either F or GT, and $|i\rangle$ and $|f\rangle$ denote the wave functions of the initial and the final states, respectively, J_i being the angular momentum of the initial state. The constant $C=6146$ s is used in the present calculations, which is determined from the $0^+\rightarrow 0^+$ Fermi transitions. The ratio of the axial-vector to vector coupling constant $|g_A/g_V|=1.239$ is used, which is extracted from the free-neutron beta decay experiments.

Two model spaces are assumed in the present calculations: the $f^n_{7/2}+f^{n-1}_{7/2}p_{3/2}$ and the $f^n_{7/2}+f^{n-1}_{7/2}(p_{3/2},p_{1/2},f_{5/2})^1$. For the former model space, we use the effective interactions obtained in Ref. 1. In that calculation,[1] the 20 two-body matrix elements and the value of the $f_{7/2}$ single-particle energy were assumed to be free parameters and were determined by means of a least-squares fitting to well-established experimental data on the low-lying energy levels. Hereafter, the calculations of any observables with this model space and the effective interactions will be referred to as calc. 1. For the extended model space, we use the effective interactions obtained in Ref. 2. The least-squares fitting procedure was also adopted but the parametrization of the effective interactions is rather complex: The effective interactions are made up of empirical matrix elements and phenomenological potentials superposed with three central interactions (we adopt version D of Ref. 2). This complexity may introduce an uncertainty into the effective interactions which should be strictly relevant to the assumed model space. Moreover, it seems that the effective interactions would not be determined uniquely by using the energy levels only. This might introduce further another uncertainty in the effective interactions in discussing the transition probabilities. In order to estimate the size of errors caused by these uncertainties, we try to use also the effective interactions proposed by the Utrecht group,[13] which are based on the G-matrix elements.[14] These two calculations with the extended model space will be referred to as calc. 2 and calc. 3, respectively, in the later discussions.

The $f^{n-2}_{7/2}j^2$ configurations are not included in the model spaces of the present calculations. The lowest-order effect introduced by such configurations would be second order for the transitions mainly determined by the $f^{n-1}_{7/2}j$ and $f^n_{7/2}$ components, respectively, in the initial- and final-state wave functions. On the other hand, first-order contributions can be obtained from such configurations for the transitions dominated by the $f^{n-1}_{7/2}j$ components in the wave functions. This means that the transitions of the former type will be consistently described by the present models within the first-order ap-

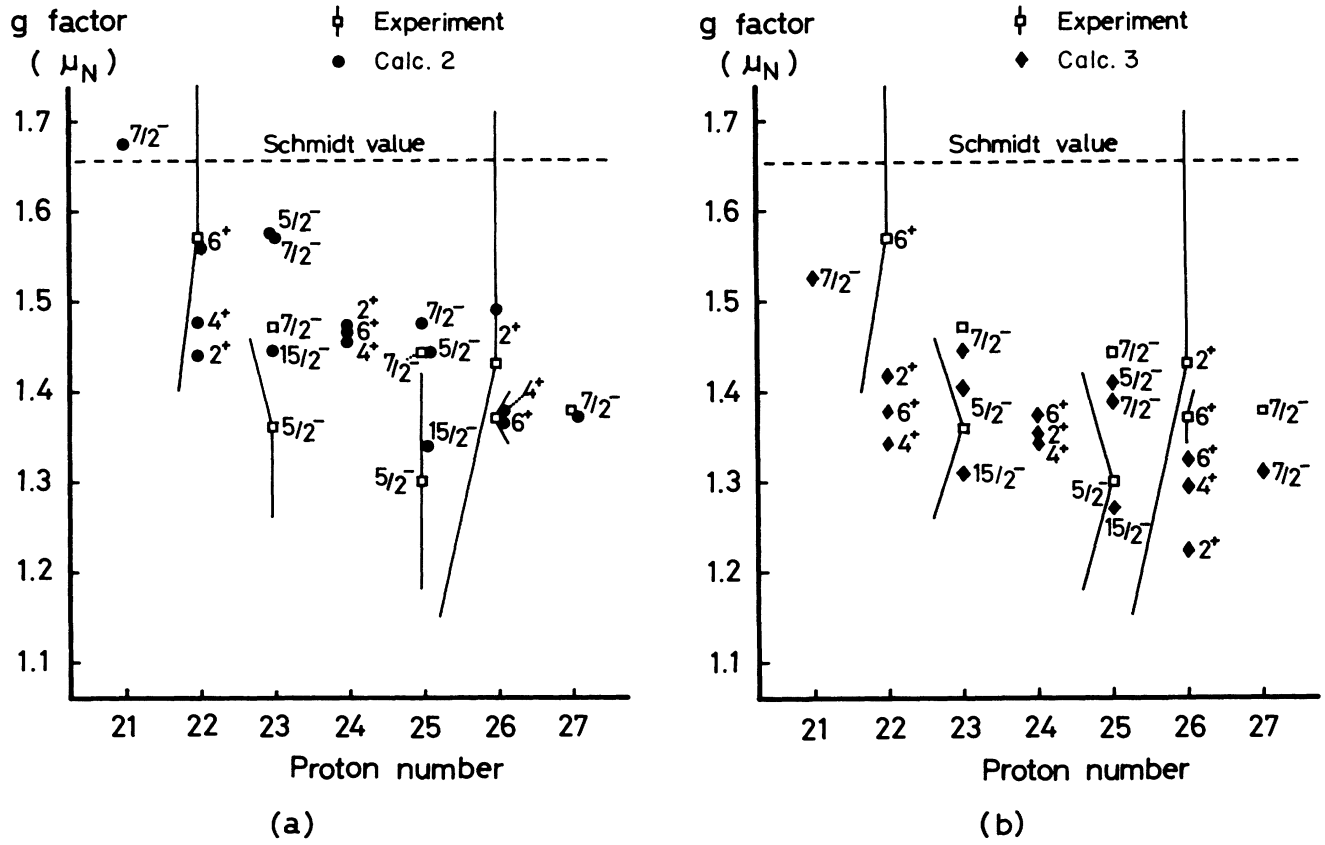

FIG. 1. Calculated and experimental (Refs. 18–23) g factors for the magnetic dipole moments of the $N=28$ isotones. The results of calc. 2 are shown by (a) and those of calc. 3 are by (b).

proximation, while the predictions for the transitions of the latter type will be less accurate.

III. RESULTS AND DISCUSSIONS

A. Magnetic moments

The low-lying levels of the $N=28$ isotones are usually described by the $\pi f_{7/2}^{p}$ configurations, and this simple model can indeed explain various properties of the isotones such as the binding energies. In this model, the $M1$ operator given by Eq. (8) is proportional to the total angular momentum J, and therefore the g factors are predicted to be the same for all levels of a given J. Mixing of the configurations to introduce the $f_{7/2} \rightarrow f_{5/2}$ excitations gives rise to a considerable change in the $M1$ matrix elements, as was shown[15] by using a first-order perturbation theory. Since the excitation of a proton is made by the interaction with another proton in the $f_{7/2}$ shell, the correction of this process cannot be renormalized into a one-particle operator but is expressed in terms of a two-particle operator.[16,17] Therefore, the configuration mixing of this type predicts both number and state dependence of the g factors. On the other hand, the excitation of a neutron is made by the interaction with a proton in the $f_{7/2}$ shell, and thus this correction is renormalized into a one-particle operator,[16,17] giving neither number nor state dependence but just uniform shift of the g factors. In the present calculations, as is expected, the proton excitation plays a significant role, giving g factors, which decrease with the number of protons, particularly for the $\frac{7}{2}^-$ and 6^+ states, and thus the experimental trend is reproduced very well as shown in Fig. 1. The state dependence is also predicted in our calculations for the g factors of the 2^+, 4^+, and 6^+ states in the even-mass isotones, being comparable with that predicted by the perturbation calculation;[17] however, there are scarce experimental data to make a detailed comparison. The contributions from the neutron excitation, on the other hand, are not so simple as expected from the perturbation calculations, and the magnitudes of their corrections tend to be smaller than those caused by the proton excitation in the heavier isotones. It is interesting to note for ^{51}V and ^{53}Mn that the largest deviation from the Schmidt value is predicted for the $\frac{15}{2}^-$ state, the highest-spin state generated by the $\pi f_{7/2}^{p}$ configurations, contrary to the expectation that the high-spin states would be purer than the lower-spin states, particularly the $\frac{5}{2}^-$ state. The difference between the two calculations, calc. 2 and calc. 3, comes mostly from the difference in the $\langle f_{7/2}^2 \mid V \mid f_{7/2} f_{5/2} \rangle_{TJ}$ matrix elements: The $T=1$ part in calc. 2 is appreciably larger than that in calc. 3, while the $T=0$ part in calc. 3 is considerably stronger than that in calc. 2. This means that the contributions from the

TABLE I. Energies and wave functions of the $J^\pi=\frac{3}{2}^-$ levels in ^{49}Sc obtained by the $f^8_{7/2}p_{3/2}$ configuration. $\bar{A}$ and C denote the antianalog and core-polarized states, respectively, where the subscript represents the angular momentum of the $f^8_{7/2}$ core state.

State	E_x (MeV) Expt.	Calc.	Amplitude $\bar{A}_0$	C_1	C_2	C_3
$3/2^-_1$	3.084	2.855	0.794	−0.275	0.115	−0.529
$3/2^-_2$		4.874	0.260	−0.243	0.662	0.660
$3/2^-_3$		5.937	−0.395	0.171	0.737	−0.521
$3/2^-_4$		7.290	−0.382	−0.915	−0.072	−0.113

two-body magnetic moment operators in perturbation theory are relatively emphasized in calc. 2, whereas those from the one-body operator are stressed in calc. 3. In either case, the small admixture of the $f_{5/2}$ component in the wave functions assures us that we obtain almost the same results as those with the perturbation calculations.

It could be said in summary that the present calculations with the $f^n_{7/2}+f^{n-1}_{7/2}(p_{3/2},p_{1/2},f_{5/2})^1$ configurations seem to provide reasonable wave functions for discussing the static $M1$ properties of the low-lying states in the $N=28$ nuclei.

B. $A=49$ nuclei

As was mentioned in the preceding section, ^{49}Sc is the most extensively studied nucleus so far as the $M1$ transition from the analog state is concerned; however, in order to be self-contained, we shall start a discussion from the simplest configuration $f^8_{7/2}p_{3/2}$. We first define a parent state (P), i.e., the ground state of ^{49}Ca, which has $T=\frac{9}{2}$ and $J^\pi=\frac{3}{2}^-$ and consists of the single basis state with $T_C=4$ and $J_C=0$, where T_C and J_C are the isospin and the angular momentum, respectively, of the $f^8_{7/2}$ core state. By using the isospin lowering operator, as in Eq. (6), we get an analog state (A). For the $J^\pi=\frac{3}{2}^-$ states in ^{49}Sc ($T=\frac{7}{2}$), we have an antianalog state ($\bar{A}$) from Eq. (3), and in addition to this state, we also have the neutron-excited states (C) given by Eq. (4), in which the isospin T_C and angular momentum J_C of the $f^8_{7/2}$ state should be recoupled. The T_C is 3 rather than 4, and J_C can take 1, 2, and 3. The basis state with $J^\pi=1^+$ is usually called the core-polarized state. Since these four basis states with $T=\frac{7}{2}$ and $J^\pi=\frac{3}{2}^-$ are almost degenerate, they are expected to be strongly mixed due to the residual interactions, and a perturbative method would no longer be applicable (if only the single-particle energies were assumed for the energy denominator, as is normally done in a perturbation calculation, the energy denominator should be zero). In Table I, the excitation energies and the wave functions are shown for the $\frac{3}{2}^-$ levels of ^{49}Sc obtained from the $f^8_{7/2}p_{3/2}$ configuration (calc. 1). It is clearly seen that the $\bar{A}$ and C states are considerably admixed in each $\frac{3}{2}^-$ level, although the lowest $\frac{3}{2}^-$ level has the largest amplitude of the $\bar{A}$ component. The $l=1$ proton stripping spectroscopic factor $(2J+1)C^2S$ leading to the lowest $\frac{3}{2}^-$ state is $4(\frac{8}{9})(0.794)^2=2.24$, being comparable with the experimental one,[24] 2.51, deduced from the ^{48}Ca(^{3}He,d) reactions. Even if we extend the model space, $f^8_{7/2}(p_{3/2},p_{1/2},f_{5/2})^1$, we have almost the same wave functions for the lowest $\frac{3}{2}^-$ state. In fact, calc. 2 and calc. 3 give the $(2J+1)C^2S$ to be 2.22 and 3.08, respectively, both of which are in qualitative agreement with the experiment. The interaction among the $f_{7/2}$ nucleons favors the C states by several MeV in energy over the $\bar{A}$ state. On the other hand, the $\tau\tau$ part of the $\langle f_{7/2}p_{3/2}\,|\,V\,|\,f_{7/2}p_{3/2}\rangle_{TJ}$ interaction depresses the $\bar{A}$ component significantly, simply because it favors the larger T_C value, as was shown by Bansal and French,[25] and is responsible for making the lowest $\frac{3}{2}^-$ state possess the largest spectroscopic factor.

Table II compares the calculated and the experimental[26,27] isovector $E2$ and $M1$ transition strengths from the

TABLE II. Calculated and experimental[a] transition strengths, $B(E2)$ in e^2fm^4 and $B(M1)$ in $10^{-2}\,\mu_N^2$, from the $\frac{3}{2}^-$ and the $\frac{5}{2}^-$ analog states of ^{49}Ca to the low-lying states in ^{49}Sc.

J^π_i	J^π_f	E_{x_f} (MeV)	Multipole	Expt.	Single-particle estimate[b]	Calc. 1	Calc. 2	Calc. 3
$\frac{3}{2}^-$	$7/2^-_{g.s.}$	0	$E2$	0.82	1.16	0.99	1.06	0.81
$\frac{3}{2}^-$	$3/2^-_1$	3.084	$M1$	2.2	128	6.75	4.38	30.7
	$5/2^-_1$	4.072	$M1$	11.2		11.1	16.1	13.1
	$1/2^-_1$	4.493	$M1$	3.6	56	27.0	0.05	10.0
	$5/2^-_2$	4.738	$M1$	10.3		10.4	3.80	0.12
$\frac{5}{2}^-$	$7/2^-_{g.s.}$	0	$M1$	39±11	107		65.4	50.6
	$3/2^-_1$	3.084	$M1$	>7.6			0.06	1.47

[a]From Refs. 26 and 27.

[b]Single-particle estimate contains the relevant isospin factors.

$\frac{3}{2}^-$ and $\frac{5}{2}^-$ analog states of ^{49}Ca to the low-lying states in ^{49}Sc. We will discuss first the transitions from the $\frac{3}{2}^-$ analog state. Nonvanishing $M1$ matrix elements between the $T=\frac{9}{2}$ and $T=\frac{7}{2}$ basis states are obtained for the transitions from the A_0 to the $\overline{A}_0$ and C_1 states, where the subscript denotes the angular momentum of the $f^8_{7/2}$ core state. The two matrix elements add destructively for the transitions from the $\frac{3}{2}^-$ analog to the first, second, and third excited $\frac{3}{2}^-$ levels, if we use the wave functions listed in Table I. Particularly for the lowest $\frac{3}{2}^-$ state, the $M1$ matrix element is almost completely cancelled, and we have obtained a strong suppression of the $M1$ strength, in good agreement both with the experiments[26] and with the previous calculations.[6-9] The qualitative feature of this $M1$ transition is not so much changed, even when the $p_{1/2}$ and $f_{5/2}$ orbits are added to the model space. In order to make our discussion more quantitative, we should include another configuration in the model space, which can generate a $|f^7_{7/2}f_{5/2}(J^\pi_C=1^+),p_{3/2}\rangle$ state. This component, if included in the $T=\frac{7}{2}$ final states, gives a much smaller $M1$ matrix element than $\overline{A}$ and C_1 do, but it becomes appreciably important after the two major contributions have cancelled each other. For the transition to the fourth excited $\frac{3}{2}^-$ state in calc. 1, the two matrix elements add constructively, so we have a large transition strength; $B(M1)=6.54\,\mu_N^2$. In calc. 2 and calc. 3, the sixth excited $\frac{3}{2}^-$ state is predicted to have the largest $B(M1)$ value; $2.39\mu_N^2$ at 8.04 MeV and 4.99 μ_N^2 at 8.42 MeV, respectively. There has been, however, no experimental measurement of such strong transitions so far.

It is apparent that the $f^8_{7/2}p_{3/2}$ configuration is not sufficient for the $\frac{1}{2}^-$ and $\frac{5}{2}^-$ states, since a considerable amount of the $p_{1/2}$ and $f_{5/2}$ proton stripping strengths have been observed experimentally[24] in exciting the low-lying $\frac{1}{2}^-$ and $\frac{5}{2}^-$ states. Therefore, the $f^8_{7/2}(p_{3/2},p_{1/2},f_{5/2})^1$ configuration should be assumed even for a qualitative discussion. The calculations with the extended model space show that the $\overline{A}$ component generated by the $f^8_{7/2}p_{1/2}$ configuration is scattered over a few low-lying $\frac{1}{2}^-$ states. In calc. 2, the lowest $\frac{1}{2}^-$ state predicted at an excitation energy of 3.937 MeV consists mainly of the $\overline{A}$ state and the $p_{1/2}$ spectroscopic factor is $2(\frac{8}{9})(0.795)^2=1.12$, in good agreement with the experimental[24] value of 1.34. This means that the $M1$ transition from the $\frac{3}{2}^-$ analog to the $1/2^-_1$ state may be interpreted mainly in terms of the $p_{3/2}\rightarrow p_{1/2}$ spin-flip transition. Furthermore, the CPS generated by the $f^8_{7/2}p_{1/2}$ configuration does not allow the $f_{7/2}\rightarrow f_{7/2}$ core transition in this case, since the $\frac{3}{2}^-$ analog state is generated by the $f^8_{7/2}p_{3/2}$ configuration only. Consequently, it is natural to expect that the $\frac{3}{2}^-$ to $1/2^-_1$ $M1$ transition must be strong. In the present calculations, however, the CPS generated by the $f^8_{7/2}p_{3/2}$ configuration is admixed appreciably in the $1/2^-_1$ state in ^{49}Sc, and thus this CPS can induce the $f_{7/2}\rightarrow f_{7/2}$ core transition. The two components, the spin-flip $p_{3/2}\rightarrow p_{1/2}$ and the spin-nonflip $f_{7/2}\rightarrow f_{7/2}$, are almost completely cancelled in calc. 2, and then we have a strongly hindered transition strength, which agrees with the experiment. This emphasizes the importance of configuration mixing in the wave function of the final state.

The first and the second excited $\frac{5}{2}^-$ states are mostly generated by the $f^8_{7/2}p_{3/2}$ configuration in calc. 2 and are predicted to be $E_x=4.151$ and 4.336 MeV. The third excited $\frac{5}{2}^-$ state with the calculated $E_x=4.753$ MeV comes mainly from the $f^8_{7/2}f_{5/2}$ configuration. The spectroscopic factor leading to this state is $6(\frac{8}{9})(0.739)^2=2.91$ in calc. 2. In calc. 3, the largest strength is predicted for the first excited $\frac{5}{2}^-$ state with 3.87. The (^{3}He,d) experiments[24] have suggested, on the other hand, that the spectroscopic factor for the $f_{5/2}$ proton transfer fragments over several low-lying $\frac{5}{2}^-$ states more strongly than the predictions. For the $M1$ transitions from the $\frac{3}{2}^-$ analog to the $\frac{5}{2}^-$ states, only the C_1 component from the $f^8_{7/2}p_{3/2}$ configuration gives a nonvanishing matrix element. Therefore, the transition strength simply depends on the size of the C_1 component in the $\frac{5}{2}^-$ state. This explains why all the models predict similar $M1$ transition strengths for the lowest $\frac{5}{2}^-$ state, and agreement between the calculations and the experiment seems quite good.

The logft values for the GT beta decays from the $\frac{3}{2}^-$ ground state of ^{49}Ca to the low-lying states of ^{49}Sc are calculated and are compared with the experiments in Table III. The same discussion just made for the isovector $M1$ transitions holds for these cases.

Within the framework of the single-particle shell model, the $M1$ transition from the $\frac{5}{2}^-$ analog to the $\frac{7}{2}^-_{\text{g.s.}}$ state (g.s. represents ground state) may be interpreted as the pure $f_{5/2}\rightarrow f_{7/2}$ spin-flip transition. In the calculations with the extended model space, various $f^8_{7/2}(p_{3/2},p_{1/2},f_{5/2})^1$ components can be admixed slightly in the $\frac{7}{2}^-_{\text{g.s.}}$ state. Among them, only the $|f^8_{7/2}(1^+),f_{5/2};\frac{7}{2}^-\rangle$ component induces the $f_{7/2}\rightarrow f_{7/2}$ core transition and gives a nonvanishing contribution to the $M1$ matrix element. Calculation 2 and calc. 3 show that the strength is reduced to be almost half as large as the single-particle estimate, in good agreement with the experiment.[27]

C. $A=50$ nuclei

No experimental data are available for γ transitions from analog states in the $A=50$ nuclei, but there are two Gamow-Teller transitions[28] from the 5^+ ground state of ^{50}Sc to the lowest 4^+ and 6^+ states of ^{50}Ti. If one assumes the lowest configurations, the 5^+ state in ^{50}Sc is considered to be a member of the $\pi f_{7/2}\nu p_{3/2}$ multiplet, while the 4^+ and 6^+ states are generated by the $\pi f^2_{7/2}$ configuration. The beta decay must proceed with the $\nu p_{3/2}\rightarrow\pi f_{7/2}$ single-particle transition, and thus this is an l- and j-forbidden transition. When the model space is extended to include the $p_{3/2}$ orbit in ^{50}Ti, then the $p_{3/2}\rightarrow p_{3/2}$ and $f_{7/2}\rightarrow f_{7/2}$ transitions become operative. The GT matrix elements obtained in calc. 1 are appreciable as shown in Table III, though they are not large enough to reproduce the experimental data yet. If we extend further the model space to include all the $p_{3/2}$, $p_{1/2}$, and $f_{5/2}$ orbits, then the $p_{3/2}\rightarrow p_{1/2}$ and $f_{7/2}\rightarrow f_{5/2}$ spin-flip transitions can be operative as well as the

TABLE III. Calculated and experimental[a] logft values.

Nuclear decay	J_i^π	J_f^π	E_{x_f} (MeV)	Experiment	Calc. 1	Calc. 2	Calc. 3
$^{49}Ca \rightarrow {}^{49}Sc$	$\frac{3}{2}^-$	$3/2_1^-$	3.085	5.038	4.281	4.363	3.869
		$5/2_1^-$	4.072	5.08	4.756	4.594	4.684
		$1/2_1^-$	4.493	5.40	4.368	4.375	3.905
		$5/2_2^-$	4.739	5.26	4.783	5.219	6.737
$^{50}Sc \rightarrow {}^{50}Ti$	5^+	4_1^+	2.675	6.52	8.5	5.552	5.254
		6_1^+	3.198	5.393	6.291	6.126	4.882
$^{51}Ti \rightarrow {}^{51}V$	$\frac{3}{2}^-$	$5/2_1^-$	0.320	4.894	4.943	4.989	4.648
		$3/2_1^-$	0.929	5.350	4.963	5.612	5.601
$^{52}V \rightarrow {}^{52}Cr$	3^+	2_1^+	1.434	5.0010	5.450	5.354	4.735
		4_1^+	2.370	7.45	5.778	5.549	6.856
		4_2^+	2.768	5.914	6.125	5.815	5.783
		2_2^+	2.965	6.305	4.929	6.769	6.316
		4_3^+	3.415	5.94	5.780	5.758	5.761
		3_1^+	3.472	6.95	5.917	7.30	6.014
		2_4^+	3.772	5.53	5.868	4.809	4.258
$^{55}Co \rightarrow {}^{55}Fe$	$\frac{7}{2}^-$	$5/2_1^-$	0.932	6.25	8.1	5.295	5.541
		$7/2_1^-$	1.317	6.88	5.080	5.881	5.458
		$5/2_2^-$	2.144	6.57	7.486	5.212	5.966
		$9/2_1^-$	2.212	6.06		5.446	5.071
		$9/2_2^-$	2.302	5.77		5.393	6.239
		$5/2_3^-$	2.578	7.36		7.71	7.46

[a]From Refs. 24, 28, 30, 32, and 35 for $A=49$, 50, 51, 52, and 55 nuclei, respectively.

above-mentioned two spin-nonflip transitions. It should be noticed that the $j=l-\frac{1}{2} \rightarrow j=l-\frac{1}{2}$ type transitions are also available but are negligibly small. Since the contributions from each single-particle transition are almost the same size, the GT matrix elements are rather sensitive to the wave functions, namely the model spaces and effective interactions employed. With this in mind, the calculated logft values shown in Table III are in satisfactory agreement with the experiments.

D. $A=51$ nuclei

The $E2$ and $M1$ transitions from the analog state of the $\frac{3}{2}^-$ ground state of ^{51}Ti to the low-lying states in ^{51}V are discussed in this subsection. The calculated results are summarized in Table IV and are compared both with the experiments[29] and with the previous calculations.[10] If one assumes the $\pi f_{7/2}^2 \nu p_{3/2}$ and the $\pi f_{7/2}^3$ configurations for ^{51}Ti and ^{51}V, respectively, the $M1$ transition is l and j

TABLE IV. Calculated and experimental[a] transition strengths, $B(E2)$ in e^2fm^4 and $B(M1)$ in $10^{-2}\,\mu_N^2$, from the $\frac{3}{2}^-$ analog state of ^{51}Ti to the low-lying states in ^{51}V.

J_f^π	E_x (MeV)	Multipole	Experiment[c]		Osnes and Warke[b] OW(3)	OW(4)	OW(5)	Present calculations calc. 1	calc. 2	calc. 3
$7/2_{g.s.}^-$	0	$E2$	0.73±0.16		0.76	0.76	0.73	0.844	0.786	0.639
$5/2_1^-$	0.320	$E2$	$0.12^{+0.10}_{-0.06}$		1.93	0.19	0.20	0.197	0.174	0.149
		$M1$	8.4 ±1.7		0.039	0.52	4.8	8.02	5.24	11.0
$3/2_1^-$	0.927	$E2$	0.08±0.03	10.0 ±1.7	0.39	0.029	0.031	0.018	0.000	0.000
		$M1$	5.1 ±1.9	0.17±0.07	0.53	0.0052	0.86	7.19	2.24	2.32
$3/2_2^-$	2.407	$E2$	0.27±0.20	4.7	0.29	0.34	0.38	0.305	0.224	0.400
		$M1$	1.5 ±0.5	$<10^{-2}$	22	57	67	14.6	9.65	46.8
$5/2_2^-$	3.077	$E2$	0.60±0.30	14	10.4	0.17	0.29	0.001	0.005	0.095
		$M1$	3.9 ±0.5	$<4\times10^{-2}$	0.36	5.3	9.8	5.87	2.30	0.746
$3/2_3^-$	3.192	$E2$	0	3.8	10.0	0.44	0.39	0.153	0.133	0.104
		$M1$	1	0	56	86	75	2.40	0.024	0.001
$3/2_4^-$	4.258	$E2$	0.39±0.25	55				0.040	0.015	0.013
		$M1$	9.4 ±1.9	$<4\times10^{-2}$				6.05	2.74	0.067

[a]From Ref. 29.
[b]From Ref. 10.
[c]When there are two possible solutions for the mixing ratio $\delta(E2/M1)$ in the experimental data, the transition rates deduced from the smaller one are shown on the left-hand side and those deduced from the larger one are on the right-hand side.

forbidden. Nonvanishing $M1$ matrix elements are easily obtained by extending the model space; the addition of the $\pi f_{7/2}^2 p_{3/2}$ configuration for ^{51}V, and similar configurations for the rest of the $N=28$ isotones were considered by Auerbach.[3] The entry shown as OW(3) in Table IV is calculated by using his wave functions. It is known, however, that the basis functions generated by the $\pi f_{7/2}^2 p_{3/2}$ configuration do not have the correct isospin, as was discussed in Sec. II, and the $\pi f_{7/2}^3 \nu f_{7/2}^{-1} p_{3/2}$ configuration must be taken into account [see Eq. (3)]. Osnes and Warke[10] examined the effects of using the good isospin wave functions on the isovector $E2$ and $M1$ transitions by using an isospin projection method, and their results are shown in the column OW(4). The basis functions involving the neutron excitation, which are defined by Eq. (4), are still ignored in their model space. They are included explicitly in calc. 1. Therefore, by the comparison of calc. 1 with OW(4), one can see the effects of the neutron-excited components in the wave functions on the isovector transitions. In OW(5), the $|\pi f_{7/2}^2(2^+),\nu f_{5/2}\rangle$ and $|\pi f_{7/2}^2(2^+),\nu p_{1/2}\rangle$ components are added artificially to the ^{51}Ti ground-state wave function so as to fit the measured GT beta decay rates for the $3/2^-_{\text{g.s.}} \rightarrow 5/2^-_1$ and $3/2^-_{\text{g.s.}} \rightarrow 3/2^-_1$ transitions. All the basis functions obtained from the $f_{7/2}^n + f_{7/2}^{n-1}(p_{3/2},p_{1/2},f_{5/2})^1$ configurations are taken into account in calc. 2 and calc. 3.

For the $E2$ transition from the analog to the $\frac{7}{2}^-$ ground state, all the models predict similar numbers. This may be due to the fact that the main components of the initial and the final states are $\pi f_{7/2}^2(0^+)\nu p_{3/2}$ and $\pi f_{7/2}^2(0^+)f_{7/2}$, respectively, and thus the $p_{3/2} \rightarrow f_{7/2}$ transition dominates in this transition. On the other hand, the $E2$ transitions to the other low-lying states must proceed through the rather small components in the wave functions, e.g., the $\pi f_{7/2}(2^+)\nu p_{3/2}$ in the initial state, since the $5/2^-_1$ and $3/2^-_1$ states contain a fair amount of the $\pi f_{7/2}^2(2^+)f_{7/2}$ component. It is easily seen from the comparison of OW(3) with OW(4) that the use of the wave functions with good isospin is crucial for the isovector $E2$ transitions. Comparing OW(4) with the other calculations using the more complicated model space, we can find that the extension of the model space does not give rise to any significant change in these transitions.

As was mentioned before, the $M1$ transitions from the $3/2^-$ analog to the $5/2^-_1$ and $3/2^-_1$ states are l and j forbidden in the lowest-configuration assumption, and it is expected that the small components admixed in the wave functions become important, contrary to the $E2$ transitions. First, we will discuss the $M1$ transition to the $5/2^-_1$ state. Comparing OW(3) and OW(4), we can see that the calculated $M1$ strength is improved to a certain extent by using the good isospin wave functions, but the experimental value is still underestimated by an order of magnitude. A substantial improvement is further obtained by OW(5), due to the $f_{5/2} \rightarrow f_{7/2}$ and $p_{1/2} \rightarrow p_{3/2}$ spin-flip transitions. On the other hand, in calc. 1 the neutron-excited components with $T_1 = T - \frac{1}{2}$ are included as the basis functions, and the $|f_{7/2}^{10}(T_1=2,J_1=1^+),\nu p_{3/2}\rangle$ component, the CPS, is admixed in the final state and can induce the strong $f_{7/2} \rightarrow f_{7/2}$ core transition. In fact, this component is the leading term in the $M1$ transition matrix element, although the mixing amplitude is fairly small. The calculations with the extended model space show that the contributions from the spin-flip transitions ($f_{7/2} \rightarrow f_{5/2}$ and $p_{3/2} \rightarrow p_{1/2}$ ones) are appreciable but are not added constructively, and thus their effects do not appear apparently in this $M1$ transition strength. It might be said that the $f_{7/2} \rightarrow f_{7/2}$ transition induced by the CPS in the final-state wave function is the major ingredient for the explanation of the $M1$ transition from the analog state to the $5/2^-_1$ state.

The $M1$ transition from the analog to the $3/2^-_1$ state may be understood almost in the same way as that for the transition to the $5/2^-_1$ state. In OW(4), the $|f_{7/2}^{10}(T_1=3,J_1=0^+),p_{3/2}\rangle$ and the $|f_{7/2}^{10}(T_1=3,J_1=2^+),p_{3/2}\rangle$ components in the final-state wave function are responsible for having nonvanishing matrix elements, but the calculated $B(M1)$ value is not sufficient to explain the experiment. The spin-flip components in OW(5) do not help drastically increase the matrix element in this case. On the other hand, a large contribution to the $M1$ matrix element can be obtained by including the neutron-excited components with $T_1 = T - \frac{1}{2}$, as shown in calc. 1. Calculation 2 and calc. 3 show that the other components, some of which induce the spin-flip contributions, do not alter significantly the result of calc. 1. This emphasizes the importance of the CPS in the $M1$ transition from the analog to the $3/2^-_1$ states. All the calculations both for the $E2$ and $M1$ transitions agree rather well with the experimental data deduced with the smaller mixing ratio $\delta(E2/M1)$. Osnes and Warke favored the smaller δ solution, because the $B(E2)$ values extracted from the larger δ were anomalously large and should be excluded.

The logft values of the GT beta decay calculated for the transitions from the $3/2^-$ ground state of ^{51}Ti to the $5/2^-_1$ and $3/2^-_1$ states of ^{51}V are shown in Table III. The neutron-excited components in the final-state wave functions play a decisive role in the GT transitions just in the same way as the $M1$ transitions. The calculations of calc. 1, calc. 2, and calc. 3 are in reasonable agreement with the experiments.

For the $M1$ transitions to the higher excited levels, the inclusion of the neutron-excited components is indispensable, since the core-polarized state C_1 is strongly fragmented over the excited states with a few MeV excitation energy, just in the same way as was discussed in the ^{49}Sc case. The $3/2^-_2$ state contains a large amount of the $\overline{A}_0$ component, the antianalog state obtained from the $f_{7/2}^{10} p_{3/2}$ configuration; in fact, the spectroscopic factor for proton stripping reactions is predicted to be 1.90 in calc. 1, 1.68 in calc. 2, and 2.37 in calc. 3, all comparable with the experimental[30] value of 2.6. In the $M1$ matrix element between the analog and the $3/2^-_2$ states, the $A_0 \rightarrow \overline{A}_0$ and $A_0 \rightarrow C_1$ contributions cancel each other to a great extent, and then we have a strong suppression of the transition strength; however, other small components, not present in the ^{49}Sc case, become relatively important and a cancellation mechanism becomes considerably complicated.

TABLE V. Calculated and experimental[a] transition strengths, $B(E2)$ in $e^2\text{fm}^4$ and $B(M1)$ in $10^{-2}\,\mu_N^2$, from the 3^+ analog state of ^{52}V to the low-lying states in ^{52}Cr.

J_f^π	E_x (MeV)	Multipole	Experiment	Prakash[b] bad T	Prakash[b] good T	Present calculations calc. 1	calc. 2	calc. 3
2_1^+	1.43	$E2$	0.51 ± 0.02	0.312	0.421	0.259	0.235	0.176
		$M1$	3.9	9.088	4.934	1.426	1.350	5.877
4_1^+	2.37	$E2$	13^{+18}_{-10}	0.022	0.032	0.003	0.146	0.020
		$M1$	$9.5^{+10.3}_{-6.8}$	0.109	0.059	1.582	1.630	0.101
4_2^+	2.77	$E2$	$4.2^{+3.9}_{-3.0}$	1.859	1.950	0.363	0.132	0.243
		$M1$	$2.2^{+1.9}_{-1.4}$	1.116	0.606	0.262	0.623	1.242
2_2^+	2.97	$E2$	<1.7	0.705	0.768	0.000	0.000	0.000
		$M1$	<0.84	73.33	39.82	8.026	0.041	0.015
4_4^+	3.41	$E2$	$0.08^{+0.26}_{-0.08}$	0.010	0.010	0.368	0.201	0.155
		$M1$	$9.5^{+3.5}_{-2.7}$	4.593	2.494	1.825	1.379	1.592

[a]From Ref. 31.
[b]From Ref. 11.

E. $A=52$ nuclei

The calculated $E2$ and $M1$ transition strengths from the analog state of the 3^+ ground state of ^{52}V to the low-lying states in ^{52}Cr are shown in Table V and are compared both with the experiments[31] and with the previous shell-model predictions.[11] The calculation of Ref. 11 takes account of the $T_1=T+\frac{1}{2}=\frac{5}{2}$ components by using the isospin projection method,[10] but it does not include the $T_1=T-\frac{1}{2}=\frac{3}{2}$ components. A few versions are presented in Ref. 11, and among them the following version is most analogous to the OW(4) and OW(5) for the $A=51$ nuclei; first doing a shell-model calculation of ^{52}Cr with the proton $f_{7/2}^4+f_{7/2}^3(p_{3/2},f_{5/2})^1$ configurations[4] and then projecting the wave functions to possess good isospin. The results of this version are presented in Table V. It is surprising to note from comparison of bad T with good T in Table V that the effect of using good isospin wave functions is not so significant as in the ^{51}V case. In another version presented in Ref. 11, the effect is not apparent either. It should be emphasized here that in the present calculations the $f_{7/2}\rightarrow f_{7/2}$ transition introduced by the $T_1=T-\frac{1}{2}=\frac{3}{2}$ components in the final-state wave functions plays an important role in the $M1$ transitions. A more detailed discussion needs further precise information on the measured transition strengths.

The calculated logft values for the GT transitions from the 3^+ ground state of ^{52}V to the low-lying states of ^{52}Cr are tabulated and compared with the experiments[32] in Table III. There seems to exist no strong contradiction between the calculations and the experiments.

F. $A\geq 53$ nuclei

In ^{53}Mn, ^{54}Fe, and ^{55}Co, the analog states of the ground states of the $N=29$ isotones are all bound states, and then the techniques used for capture reactions such as (p,γ), which are powerful to deduce the γ-transition rates for the unbound states, can no longer be applied to these cases. On the other hand, the analog states of the excited states of the $N=29$ isotones can be unbound, and a few experiments have been done[33] by using the capture reactions. Table VI compares the calculated and experimental $E2$ and $M1$ transition strengths from the analog state of the $1/2_1^-$ state of ^{53}Cr to the low-lying states in ^{53}Mn. According to the (d,p) reactions[34] on ^{52}Cr, the low-lying $\frac{1}{2}^-$ states in ^{53}Cr have a large fraction of the $\nu p_{1/2}$ strength, and the spectroscopic factor for the lowest $\frac{1}{2}^-$ state is 0.71, suggesting that $\pi f_{7/2}^4\nu p_{1/2}$ is the principal configuration for this state. The calculated values are 1.14 with calc. 2 and 1.06 with calc. 3, being slightly larger than the experiment.

The $M1$ transition from the $1/2_1^-$ analog to the $3/2_1^-$ state is forbidden in the single-particle shell model, since the initial and the final states are generated by the $f_{7/2}^{12}p_{1/2}$ and the $f_{7/2}^{13}$ configurations, respectively. In the extended shell model, a considerable amount of the $f_{7/2}^{12}(J'\neq 0)\times\nu(p_{3/2},f_{5/2})^1$ components are admixed in the $\frac{1}{2}^-$ state of ^{53}Cr, and an appreciable amount of the $f_{7/2}^{12}(p_{3/2},p_{1/2},f_{5/2})^1$ components are contained in the low-lying states of ^{53}Mn. Then, all the $p_{3/2}\rightarrow p_{3/2}$, $p_{3/2}\rightarrow p_{1/2}$, $f_{7/2}\rightarrow f_{7/2}$, and $f_{7/2}\rightarrow f_{5/2}$ transitions become operative in this $M1$ transition. There occurs a cancellation among them, and we can always have a small $M1$ matrix element. Calculation 2 agrees with the experiment very well.

The $3/2_2^-$ state of ^{53}Mn has most of the $\overline{A}_0$ component obtained from the $f_{7/2}^{12}p_{3/2}$ configuration. The calculated $p_{3/2}$ proton stripping strengths are 2.24 in calc. 1, 1.95 in calc. 2, and 2.23 in calc. 3, slightly larger than the experi-

TABLE VI. Calculated and experimental[a] transition strengths, $B(E2)$ in $e^2\text{fm}^4$ and $B(M1)$ in $10^{-2}\,\mu_N^2$, from the $\frac{1}{2}^-$ analog state of ^{53}Cr to the low-lying states in ^{53}Mn.

J_f^π	E_x (MeV)	Multipole	Experiment	Calc. 2	Calc. 3
$5/2_1^-$	0.38	$E2$	1.3	0.100	0.281
$3/2_1^-$	1.29	$M1$	1.8	1.80	0.566
$3/2_2^-$	2.41	$M1$	3.6	32.2	61.4
$1/2_1^-$	2.67	$M1$	7.2	22.6	8.36

[a]From Ref. 33.

mental value[34] of 1.45 extracted from the (^{3}He,d) reactions. Thus, the $M1$ transition from the $\frac{1}{2}^-$ analog to the $3/2_2^-$ state may proceed mainly via the spin-flip $p_{1/2}\rightarrow p_{3/2}$ transition. Moreover, if one assumes that the $1/2_1^-$ state of ^{53}Cr comes from only the $f_{7/2}^{12}p_{1/2}$ configuration, the CPS generated by the $f_{7/2}^{12}p_{3/2}$ configuration, which is admixed in the $3/2_2^-$ state of ^{53}Mn, does not induce the $f_{7/2}\rightarrow f_{7/2}$ core transition. This is in contrast to the $M1$ transitions from the $\frac{3}{2}^-$ analog to the $\frac{3}{2}^-$ states with the largest spectroscopic factors in ^{49}Sc and ^{51}V, in which the CPS gives rise to the important cancellation. It is therefore expected in this naive picture that the $1/2_1^-\rightarrow 3/2_2^-$ $M1$ transition in ^{53}Mn must be considerably strong. In the present calculations, this spin-flip $p_{1/2}\rightarrow p_{3/2}$ transition is in fact the major component in the $M1$ matrix element, and the $f_{7/2}\rightarrow f_{7/2}$ transition, which is induced by the CPS of the $f_{7/2}^{12}p_{1/2}$ configuration admixed in the final $3/2_2^-$ state, does cancel the $p_{1/2}\rightarrow p_{3/2}$ contribution. The cancellation effect is not perfect, however, as can be seen from Table VI. This may be understood by the fact that the calculations overestimate the spectroscopic strengths both for the $1/2_1^-$ state of ^{53}Cr and for the $3/2_2^-$ state of ^{53}Mn and consequently overestimate the $p_{1/2}\rightarrow p_{3/2}$ spin-flip contribution.

For the $A=55$ nuclei, electron capture decay data for the ^{55}Co$\rightarrow$ ^{55}Fe transition are available, and comparison of the experiments[35] with the calculations is made in Table III. The $5/2_1^-$ and $5/2_2^-$ levels in ^{55}Fe have been strongly populated in the single-neutron transfer reactions with the transferred angular momentum of $l_n=3$. The spectroscopic strengths for these levels extracted from the (d,p) experiments[35] are 3.9 and 0.92, respectively. The calculated spectroscopic strengths for the $5/2_1^-$ and $5/2_2^-$ levels are 3.37 and 0.88 in calc. 2, and 3.73 and 0.53 in calc. 3, respectively, being in good agreement with the expeirments. Since the ground state of ^{55}Co consists mainly of the $f_{7/2}^{15}$ component and the low-lying states of ^{55}Fe are composed of several $f_{7/2}^{14}j$ components, the $f_{7/2}\rightarrow f_{5/2}$ spin-flip transition is expected to be important. It is in fact the leading term in the $7/2_{\text{g.s.}}^-\rightarrow 5/2_{1,2}^-$ and the $7/2_{\text{g.s.}}^-\rightarrow 9/2_{1,2}^-$ transitions; however, the other components, particularly the $f_{7/2}\rightarrow f_{7/2}$ core transition, cannot be neglected. The two $f\rightarrow f$ contributions are added in phase in the $7/2_{\text{g.s.}}^-\rightarrow 5/2_{1,2}^-$ and $9/2_1^-$ transitions, and a cancellation occurs in the $7/2_{\text{g.s.}}^-\rightarrow 9/2_2^-$ transition. For the $7/2_{\text{g.s.}}^-\rightarrow 7/2_1^-$ transition, the $p_{3/2}\rightarrow p_{3/2}$ transition plays a decisive role, since the $|f_{7/2}^{14}(T_1=1,J_1=2^+),\nu p_{3/2}\rangle$ is the major component in the $7/2_1^-$ state of ^{55}Fe and the $|f_{7/2}^{14}(2^+),p_{3/2}\rangle$ component is admixed appreciably in the $7/2_{\text{g.s.}}^-$ of ^{55}Co. The $7/2_2^-$ state in ^{55}Fe would come mainly from the $f_{7/2}^{13}(p_{3/2},p_{1/2},f_{5/2})^2$ configuration, as is suggested from the two-neutron transfer reactions, so that it is beyond the scope of the present analysis.

IV. SUMMARY AND CONCLUSION

We have discussed the isovector $E2$ and $M1$ transitions from the isobaric analog states of the $N=29$ isotones to the low-lying states in the $N=28$ isotones and the Gamow-Teller beta decay matrix elements between the states of the $N=28$ and $N=29$ nuclei. The shell-model wave functions obtained from the $f_{7/2}^{n-1}j$ configurations are assumed for the $N=29$ isotones and those from the $f_{7/2}^n+f_{7/2}^{n-1}j$ are used for the $N=28$ isotones. Two calculations with the different configurations have been made; one with $j=p_{3/2}$ only and the other with $j=p_{3/2}$, $p_{1/2}$, and $f_{5/2}$, by using the effective interactions relevant to each assumed model space. They have been compared with the previous shell-model calculations[10,11] of the isovector transitions, in which the neutron-excited components involving isospin- and spin-recoupling were not taken into account. The role of the various wave-function components entering into the transition matrix elements has been studied stepwise.

Magnetic dipole moments of the $N=28$ isotones are well interpreted by the spin-flip $f_{7/2}\rightarrow f_{5/2}$ transition caused by the small admixture of the $f_{5/2}$ components in the wave functions. The present shell-model calculations predict both number and state dependence for the g factors and agree with the perturbation calculations,[16,17] both of which emphasize the importance of the proton excitation from the $f_{7/2}$ to $f_{5/2}$ orbit.

For the isovector $E2$ transitions allowed in the single-particle shell model, e.g., the transition from the analog of the $\frac{3}{2}^-$ ground state of the $N=29$ isotones to the $\frac{7}{2}^-$ ground state in the $N=28$ isotones, the major components of the wave functions which can induce the $p_{3/2}\rightarrow f_{7/2}$ transition play a decisive role. For the other $E2$ transitions which are forbidden in the framework of the single-particle shell model, rather small components contribute to the matrix elements and the use of the good isospin wave functions becomes crucial. The results for the isovector $E2$ transitions in ^{51}V confirm the conclusion of the previous calculations by Osnes and Warke.[10]

For the isovector $M1$ transitions, the $f_{7/2}\rightarrow f_{7/2}$ core transition, which can be introduced by the neutron-excited configurations in the wave functions of the $N=28$ nuclei, becomes of primary importance, in sharp contrast to the previous calculations by Osnes and Warke.[10] The $f_{7/2}\rightarrow f_{7/2}$ transition alone can explain roughly the l and j forbidden $M1$ and GT transition matrix elements in ^{51}V and also plays a significant role in the $M1$ transitions to higher-lying states. It can easily be shown that the fragmentation of the $M1$ strengths is largely determined by the amount of the wave-function components which induce the $f_{7/2}\rightarrow f_{7/2}$ transition. The suppression of the $M1$ transition from the analog state to the low-lying state with the largest spectroscopic factor can be explained roughly by the cancellation effects between the $A\rightarrow\overline{A}$ and $A\rightarrow C_1$ components in the transition matrix elements, as was already indicated by the previous studies.[6-9] It should be mentioned, however, that a perturbative calculation can no longer be applicable, since the various components of $\overline{A}_J$ and C_J are admixed rather strongly in the wave functions, and moreover the cancellation in the $M1$ matrix elements makes the other small contributions, e.g., the $p_{3/2}\rightarrow p_{1/2}$ transition, relatively significant.

We conclude that the model space and the effective in-

teractions adopted in the present calculations give a reasonable description for the isovector $E2$ and $M1$ transition and the GT beta decay matrix elements as well as the energy levels and other spectroscopic properties published[1,2] so far. More qualitatively, there still remains some fluctuations of the calculated values around the experimental ones, suggesting that the next-order wave function components should be taken into account. An analysis[36] of the GT matrix elements for the whole $1f_{7/2}$ region has shown that the one-particle excitation from the $f_{7/2}$ to $f_{5/2}$ orbit can account for the experiments qualitatively, but at least the two-particle excitations from the $f_{7/2}$ to the higher orbits are needed for a quantitative fit to the experiments.

ACKNOWLEDGMENTS

We thank Professor T. Oda for his cooperation in the early stages of the present studies. The numerical calculations were carried out with the HITAC M-682H/M-680H system at the Computer Centre of the University of Tokyo.

[1]A. Yokoyama, T. Oda, and H. Horie, Prog. Theor. Phys. **60**, 427 (1978); Phys. Lett. **99B**, 5 (1981); T. Iwamoto, H. Horie, and A. Yokoyama, Phys. Rev. C **25**, 658 (1982).
[2]A. Yokoyama and H. Horie, Phys. Rev. C **31**, 1012 (1985).
[3]N. Auerbach, Phys. Lett. **24B**, 260 (1967).
[4]K. Lips and M. T. McEllistrem, Phys. Rev. C **1**, 1009 (1970).
[5]E. Osnes, in *Proceedings of the Topical Conference on the Structure of $1f_{7/2}$ Nuclei*, edited by R. A. Ricci (Editrice Compositori, Bologna, 1971), p. 79.
[6]G. F. Bertsch and J. Damgaad, Phys. Lett. **23**, 342 (1966).
[7]S. Maripuu, Phys. Lett. **31B**, 181 (1970).
[8]M. Hirata, Phys. Lett. **32B**, 656 (1970).
[9]S. D. Bloom, J. B. McGrory, and S. A. Moszkowski, Nucl. Phys. **A199**, 369 (1973).
[10]E. Osnes and C. S. Warke, Nucl. Phys. **A154**, 331 (1970).
[11]M. Prakash, Nucl. Phys. **A304**, 173 (1978).
[12]M. Morita, *Beta Decay and Muon Capture* (Benjamin, Reading, Massachusetts, 1973).
[13]A. G. M. van Hees and P. W. M. Glaudemans, Z. Phys. A **303**, 267 (1981).
[14]T. T. S. Kuo and G. E. Brown, Nucl. Phys. **A114**, 241 (1968).
[15]H. Noya, A. Arima, and H. Horie, Prog. Theor. Phys. Suppl. **8**, 33 (1958).
[16]A. Arima, in *Proceedings of the Topical Conference on the Structure of $1f_{7/2}$ Nuclei*, edited by R. A. Ricci (Editrice Compositori, Bologna, 1971), p. 385.
[17]H. Horie, J. Phys. Soc. Jpn. Suppl. **34**, 461 (1973).
[18]E. Bozek, B. Haas, B. Ingarden-Dutkiewicz, K. Krolas, J. C. Merdinger, J. Styczen, and J. P. Vivien, Nucl. Phys. **A266**, 457 (1976).
[19]T. Nomura, J. Phys. Soc. Jpn. Suppl. **34**, 619 (1973).
[20]S. H. Sie, G. G. Frank, and H. C. Evans, Nucl. Phys. **A243**, 1 (1975).
[21]G. K. Hubler, H. W. Kugel, and D. E. Murnick, Phys. Rev. Lett. **29**, 662 (1972).
[22]R. Hensler, J. W. Tape, N. Benczer-Koller, and J. R. MacDonald, Phys. Rev. Lett. **27**, 1587 (1971).
[23]P. T. Callaghan, M. Kaplan, and N. J. Stone, Nucl. Phys. **A201**, 561 (1973).
[24]M. L. Halbert, Nucl. Data Sheets **24**, 175 (1978).
[25]R. K. Bansal and J. B. French, Phys. Lett. **11**, 145 (1964).
[26]M. Adachi and H. Taketani, J. Phys. Soc. Jpn. **35**, 325 (1973).
[27]F. S. Dietrich, S. D. Bloom, and D. W. Heikkinen, Nucl. Phys. **A259**, 75 (1976).
[28]D. E. Alburger, Nucl. Data Sheets **42**, 369 (1984).
[29]C. Gaarde, K. Kemp, Y. V. Naumov, and P. R. Amundsen, Nucl. Phys. **A143**, 497 (1970).
[30]R. L. Auble, Nucl. Data Sheets **23**, 163 (1978).
[31]G. J. Faini, R. L. Ezell, E. L. Wills, H. L. Scott, and W. G. Love, Nucl. Phys. **A212**, 541 (1973).
[32]J. R. Beene, Nucl. Data Sheets **25**, 235 (1978).
[33]S. Maripuu, Nucl. Phys. **A149**, 593 (1970).
[34]L. K. Peker, Nucl. Data Sheets **43**, 481 (1984).
[35]Z. Enchen, H. Junde, Z. Chunmei, Lu Xiane, and W. Lizheng, Nucl. Data Sheets **44**, 463 (1985).
[36]H. Miyatake, K. Ogawa, T. Shinozuka, and M. Fujioka, Nucl. Phys. **A470**, 328 (1987).